Climatic Change (2018) 148:235–247
https://doi.org/10.1007/s10584-018-2174-6

Maps of wind hazard over South Eastern South America considering climate change

L. Augusto Sanabria[1,2,3] · **Andrea F. Carril**[1,2,4]

Received: 7 August 2017 / Accepted: 2 March 2018 / Published online: 18 March 2018

Abstract Wind is one of the most dangerous natural phenomena for the built environment in South Eastern South America. The hazard posed by wind depends on the extreme wind speeds on the surface and can be quantified by calculating the Average Recurrence Interval—more commonly known as return period—of these winds. Maps of return period of extreme wind speeds are used by planning authorities to enforce appropriate standards for infrastructure construction in most countries of the world. These maps are usually built up from wind speeds recorded at a network of weather stations. In some countries, however, the quality of the records is poor or the stations have not been in operation for long enough to give appropriate data for wind hazard studies. In this paper, we discuss an alternative approach based on wind speeds calculated by climate models. The approach provides longer datasets and facilitates assessment of the impact of climate change on wind hazard, a matter of great of importance for planning and emergency authorities. Map quality is evaluated by comparing results from the climate simulations with results from reanalysis. The comparison shows that the climate simulations produce results close enough to the reanalysis and hence they can be used for wind hazard assessment. The results also show that we could expect little variation in wind hazard in South Eastern South America during most of this century.

Electronic supplementary material The online version of this article (https://doi.org/10.1007/s10584-018-2174-6) contains supplementary material, which is available to authorized users.

✉ L. Augusto Sanabria
augusto_sf@hotmail.com

[1] Facultad de Ciencias Exactas y Naturales, FCEN/UBA, Universidad de Buenos Aires, Buenos Aires, Argentina

[2] CONICET - Universidad de Buenos Aires, Centro de Investigaciones del Mar y la Atmósfera (CIMA/CONICET-UBA), Buenos Aires, Argentina

[3] CIMA, Ciudad Universitaria, Intendente Güiraldes 2160, Pabellón 2, Piso 2, Buenos Aires, Argentina

[4] Instituto Franco-Argentino sobre Estudios de Clima y sus Impactos (UMI 3351-IFAECI/CNRS-CONICET-UBA), Buenos Aires, Argentina

1 Introduction

We are living in a changing world where the climate change projections and its impact on society and ecosystems have become a key issue for decision makers. South Eastern South America (SESA) is the most densely populated region in South America, sensitive to climate variability and change, with potential consequences for water resources and agricultural activities. To analyze climate change scenarios over South America with their underlying uncertainty, coordinated multi-regional climate models (RCMs) integrations have been done in the framework of both CLARIS EU-FP6 (Boulanger et al. 2010) and CLARIS-LPB EU-FP7 (Boulanger et al. 2016) projects. The experimental set up follows the CORDEX Protocol Phase I (Giorgi et al. 2009). A number of recent papers discuss projected changes in temperature, precipitation and drought in SESA using CLARIS simulations, including considerations about extremes and feedbacks between the continental surface and the atmosphere (López-Franca et al. 2016; Menéndez et al. 2016; Carril et al. 2016; Solman 2016; Sánchez et al. 2015; Cavalcanti et al. 2015; Solman et al. 2013; Carril et al. 2012; Menéndez et al. 2010). Nevertheless, there is a lack of information regarding surface wind sensitivity to climate change.

Extreme near-surface wind, chiefly associated with structured storm circulations (Zipser et al. 2006), is one of the most damaging natural phenomena for the built environment in SESA (Durañona 2015; Pita and Schwarzkopf 2016; Ferreira and Nascimento 2016). In particular, the new regulations for design of structures in Argentina propose wind loads corresponding to return periods of 1700 years for structures types III and IV (Natalini et al. 2016). Neither the set of regional climate models from CLARIS and CLARIS-LPB projects nor other datasets have ever been used to study wind hazard over SESA. Therefore, the first objective of this work is to evaluate the performance of CLARIS-LPB simulations on reproducing surface winds for wind hazard assessment. The scarcity of quality wind speed records with sufficient spatial and temporal resolution is a limitation for determining wind characteristics in the SESA region; therefore, we validate the results against reanalysis data. The second goal of this study is the assessment of potential change of wind hazard in a warmer climate, a subject of relevance for planning and emergency authorities in SESA. Estimation of wind hazard from numerical models is a novel issue in this part of the world, and it is an important contribution to the revision of wind loading standards going on in some countries of the region. Review of the wind hazard literature considering climate change have been performed by Rockel and Woth (2007), Kunz et al. (2010), Pryor et al. (2012), Cheng et al. (2012), Wang et al. (2013).

The paper is organized as follows. A description of models, data and methodology are provided in "Section 2." "Section 3" shows maps of return period of near-surface wind speed estimated from the ERA-Interim reanalysis (benchmark). "Section 4" assesses the capability of models to represent the benchmark wind hazard. Climate change projections of wind hazard are in "Section 5." Conclusions and plans for future works are in "Section 6."

2 Data and methodology

The region of study is defined by latitude 22°S and 38°S; and longitude 42°W and 67°W. It comprises Northern Argentina, Southern Paraguay, Southern Brazil, and Uruguay (see Fig. 1). We are interested in near-surface wind speed extracted from the CLARIS-LPB simulations. This project uses wind data from reanalysis and from two types of CLARIS

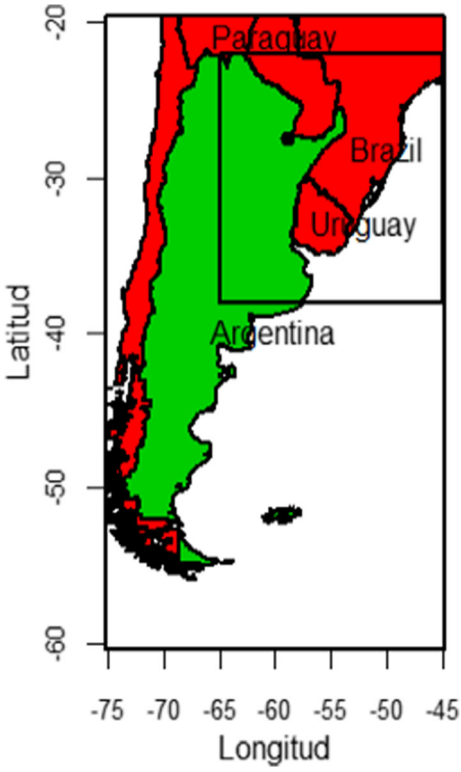

Fig. 1 Map of Southern South America. The black square shows the SESA region. The black dot shows the city of Resistencia in northern Argentina

simulations namely: (i) Reanalysis-driven simulations (hereafter, "perfect boundary condition" PBC) Giorgi (2006) and (ii) the data set of "imperfect boundary condition" (hereafter, IBC) driven by GCMs from the Climate Model Intercomparison Project (CMIP3) under the SRES A1B emission scenario (Nakicenovic et al. 2000). The complete matrix of CLARIS-LPB experiments including the RCMs and boundary conditions together with the periods of integration are presented in Table 1. Unfortunately, only four of the six simulations calculate 10 m wind speed: REMO, RCA, PROMES, and LMDZ, these are the climate simulations used in this project.

Table 1 The CLARIS-LPB matrix of experiments (Solman et al. 2013)

RCM	Institution	Boundary Conditions	1991–2010	1961–2100
REMO	MPI-CSC Germany	ERA-Interim	X	
REMO	MPI-CSC Germany	EC5OM		X
RCA	Rossby Center Sweden	ERA-Interim	X	
RCA	Rossby Center Sweden	EC5OM		X
PROMES	UCLM Spain	ERA-Interim	X	
PROMES	UCLM Spain	HadCM3-Q0		X
LMDZ	IPSL France	ERA-Interim	X	
LMDZ	IPSL France	IPSLA1B		X

Initially, we assess the skill of the reanalysis-driven CLARIS simulations in reproducing wind hazard by comparing with wind hazard calculated from reanalysis as discussed in "Section 3." To assess the impact of climate change on wind hazard we use the set of IBC experiments.

It is important to point out that in this study, we model only synoptic winds, modeling non-synoptic winds is beyond the scope of this project, interested readers can refer to the works of Cheng et al. 2012; Cechet et al. 2012; Ferreira and Nascimento 2016 or Holmes 2007. Specifically, we consider *mean* or time-averaged synoptic wind speed at 10 m height over open, flat terrain (Gatey 2011; Cvitan 2003). In this paper, we refer to this type of wind simply as "wind speed" (ws).

2.1 Wind speeds from ERAi

Near-surface winds in SESA exhibit subtropical climate characteristics produced by large scale circulation, contrasting oceanic boundary conditions, landmass distribution, synoptic weather systems, and/or monsoonal effects (Garreaud et al. 2009). The spatial variability of the wind speed over this region is provided by numerical models. In this study, we also use wind speeds calculated by reanalysis, in particular, we use the reanalysis provided by ERA-Interim (hereafter ERAi) a product of the European Centre for Medium Range Weather Forecast ECMWF (Dee et al. 2011). This is the most up-to-date reanalysis based on the Integrated Forecast System, the main weather forecasting tool of the ECMWF. Reanalysis-based wind hazard is used in this project as the benchmark to compare our CLARIS simulations against. ERAi horizontal resolution is about 0.5° and the data set spans from 1979 to the present; it includes four wind samples per day (at 0, 6, 12, and 18 h), and we use the maximum of the four, i.e., we use maximum daily wind speed.

The quality of the reanalysis-calculated wind speed is the main source of uncertainty in this project. Although it has been evaluated in other parts of the world by Bao and Zhang (2013), Brower (2013), Liléo et al. (2013) and Song et al. (2015), to our knowledge, no studies of the quality of the reanalysis-based wind speed over SESA have been published to date.

2.2 Methodology

Wind hazard is quantified by using the concept of average recurrence interval, more commonly known as return period (RP). If a given value of wind speed at certain location, termed "return level" is exceeded with probability "p" on average once a year, the RP corresponding to this return level is 1/p years (Coles 2001). The concept of RP is particularly useful to assess the long-term tendency of extreme values, the values of interest in hazard studies. In this case, we fit an extreme-value distribution to the tail of the wind time series and extrapolate well beyond the range of the available data (Coles 2001).

Since we are using maximum daily wind speed, the recommended extreme value distribution for this case is the Generalized Pareto Distribution (GPD) (Coles 2001; Holmes and Moriarty 1999). One of the problems fitting the GPD is the selection of the appropriate threshold. In this study, the automatic procedure to select the appropriate threshold to fit the GPD developed by Sanabria and Cechet (2007) will be used. Calculation of return periods is not complete without the computation of the confidence interval (CI). This is the range of values in which the true value of the RP level lies for a given probability. In this work, we use the profile-likelihood method to calculate the CI for a 95% probability; this method allows the analyst to consider the asymmetry of the distribution (Gilleland and Katz 2005).

To illustrate the methodology consider the maximum daily wind speed at Resistencia, a city located in northeast Argentina. The wind speed covers 20 years of data and it is extracted from the ECMWF reanalysis at the cell closest to the location of Resistencia, see Fig. 1. Figure 2 presents the RP of wind speed calculated via the GPD (black curve). The red circles are the RP calculated from the wind speeds and provide an easy way to check the quality of the GPD model. Notice that the GPD curve fits well the data and all the modeled RPs are within the 95% CI (more details about the methodology are presented in the Supplementary Material submitted with this paper).

To generate the *map* of RP from simulations, we interpolated the climate simulations to a common 0.5° grid (using triangulation-based linear interpolation) and extracted the maximum daily wind. The curve of RP was calculated for each of the 1632 cells in the common grid over the SESA domain. To maintain consistency between ERAi and climate simulations (for current climate conditions), the RP curve was calculated using the same 20-year period (1991–2010); we assume that the time series of wind speed is stationary over this interval, i.e., the parameters of the distribution do not change during this period. The main drivers for non-stationary conditions are climate change and seasonal characteristics (Katz 2013); the former will be discussed in "Section 5," the latter in "Section 3.1."

Results from both the models and ERAi are summarized in maps of wind speed for a given RP by calculating and plotting the wind speed for the required RP in each cell of the grid.

3 Maps of return period of wind speeds

Figure 3 shows maps of wind speed corresponding to a 50-year return period calculated from the ERAi data set. The bottom maps show the corresponding confidence interval (at 95%). Values higher than 15 m/s over Uruguay and over vast regions of Argentina (Buenos Aires and along two axis from Uruguay and Buenos Aires to central-western Argentina) can be observed. On the other hand, relatively low values of wind can be seen in the south of Brazil, Paraguay, and in the northeast of Argentina (Misiones province). Panels *b* and *c* in Fig. 3 present the range of variation of the 95% CI.

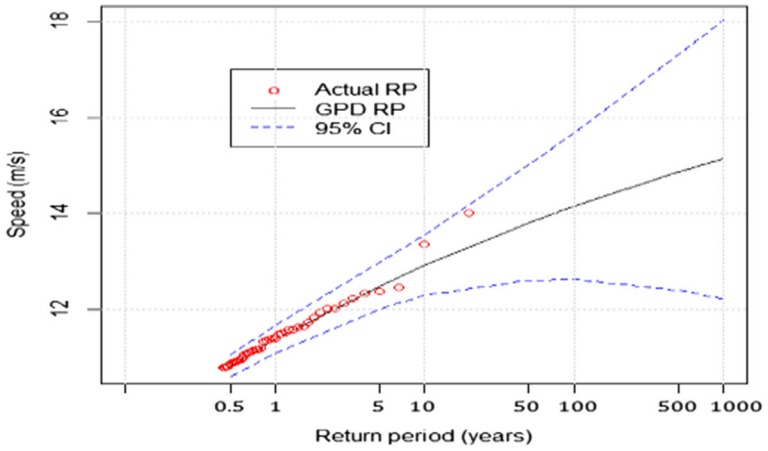

Fig. 2 Curve of RP of wind speed at Resistencia (black line) with 95% CI (blue dashed lines). The black line is calculated by a GPD, the red circles are calculated from the wind speed values

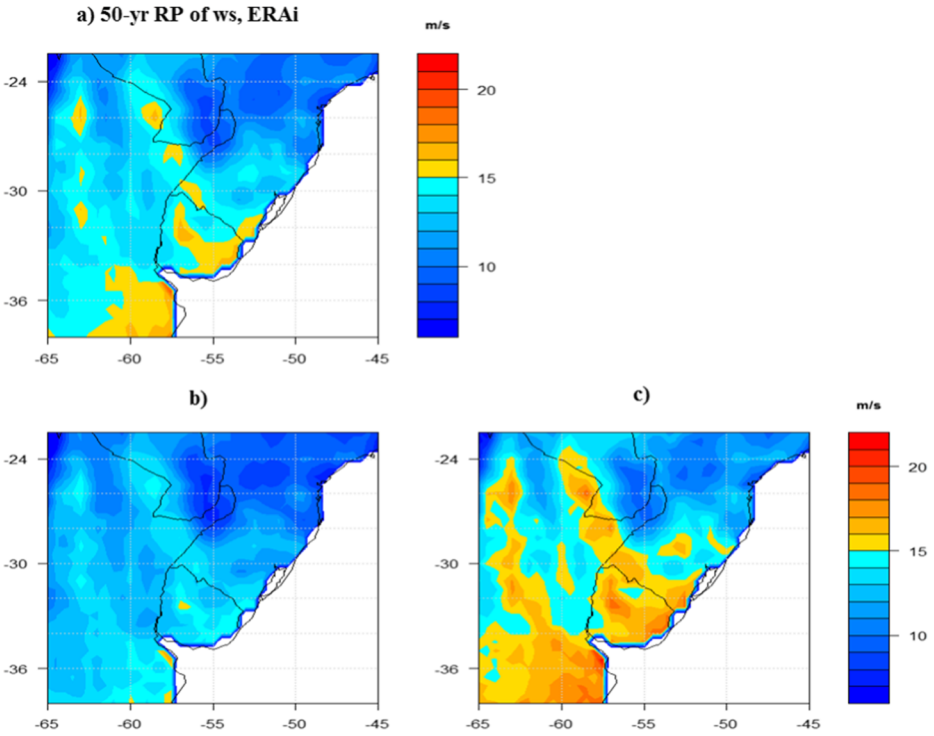

Fig. 3 Wind speed from ERAi corresponding to **a** 50-year return period, **b** lower limit of the 95% confidence interval, and **c** upper limit of the 95% confidence interval. Units are m/s

The curve of Fig. 2 shows a steady increase of wind speeds for longer RP; they do not, however, take into account the impact of climate change; this can substantially modify the long-term tendency of wind speeds. It is particularly important to examine extreme values: in some cases, mean and standard deviation of the wind distributions remain static while extremes tend to increase (Gilleland and Katz 2011). The increase in extremes means that events that used to occur with a 20-year RP are now having a recurrence of 10 years (Zhang and Zwiers 2013). Maps of wind speed considering climatic change are presented in "-Section 5" (more maps are provided in the Supplementary Material).

3.1 Sensitivity of wind speed to season

In order to study the sensitivity of SESA wind speed for a given season, the procedure was repeated splitting the ERAi data on seasonal basis (to ensure that we have enough data to fit the GPD, the amount of data was increased to 36 years by considering the period 1979–2015). The seasons in Fig. 4 are defined as DJF (December–January–February, austral summer), MAM (March–April–May, austral autumn), JJA (June–July–August, austral winter), and SON (September–October–November, austral spring), respectively. The maps of the 50-year return period of wind speed in Fig. 4 look very similar to the map presented in Fig. 3a indicating that return values of synoptic winds are not very sensitive to the time of the year. In other words, strong winds in SESA can happen any season of the year.

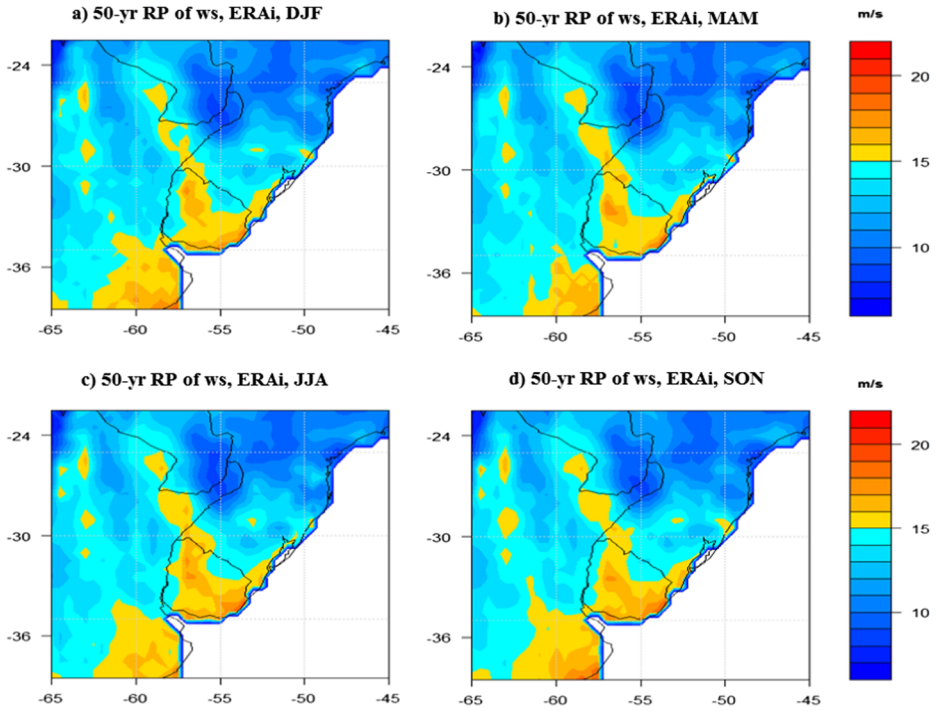

Fig. 4 Wind speed from ERAi for a 50-year RP. **a** DJF. **b** MAM. **c** JJA. **d** SON. Units are m/s

4 Capability of RCMs to simulate wind speeds

4.1 Individual models' performance

Applying the methodology described in "Section 3," maps of wind speed for the 50-year return period have been calculated from the RCMs-PBC data sets. The quality of the results is assessed by comparing against ERAi. Figure 5 provides a graphical summary of how well the 50-year RP of RCMs-PBC matches the reference wind speed (ERAi) by using a Taylor Diagram (Taylor 2001). The parameters displayed are root mean square difference (RMS), correlation coefficients (R) and standard deviation (STD). The statistics are calculated over the full SESA domain. Maps of wind speed from RCMs-PBC experiments for a 50-year RP (Fig. 6) complement the information presented in the Taylor diagram.

In term of spatial anomalies, REMO is the model that better compares with the benchmark (Fig. 5) with spatial correlation of about 0.95, RMS of about 2.1 m/s and STD about 6.1 m/s. Correlation and RMS values calculated from RCA and LMDZ wind speeds are close to the benchmark than those from REMO. On the other hand, PROMES is the model with the worst performance. Similar results have been reported by Carril et al. (2012, 2016) for temperature and precipitation, especially during the summertime. A useful technique to reduce the model internal biases is by considering results from the multi-model ensemble (Solman et al. 2013; Carril et al. 2012). The RP of the ensemble (calculated from all wind speeds of the four individual models) presents the results closest to the benchmark as shown by the purple dot.

Maps of 50-year return period of wind speed from the RCMs-PBC experiments (Fig. 6) complement the information provided in the Taylor diagram. All models capture the main

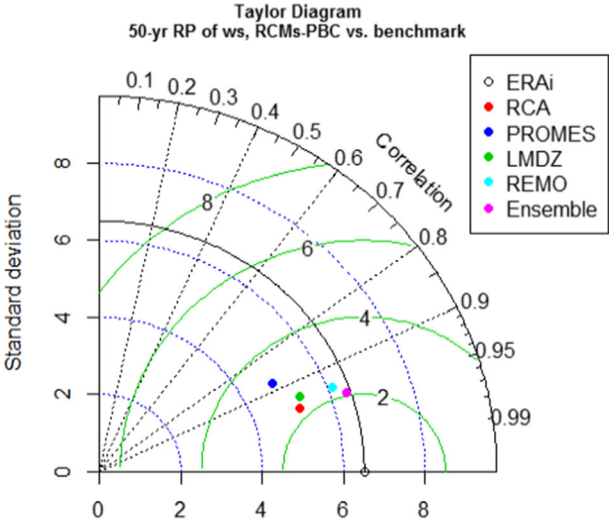

Fig. 5 Taylor diagram illustrating the skill of individual models driven by perfect boundary conditions to reproduce the ERAi maps of wind speed (for a 50-year RP). The diagram is built from three statistics: the standard deviation (vertical axis), the correlation coefficient (axial axis) and the mean root square error (concentric green circles). The filled dots are PROMES (blue), RCA (red), LMDZ (green), REMO (light-blue), and Ensemble (purple), while ERAi (the benchmark) is the empty black circle at the bottom

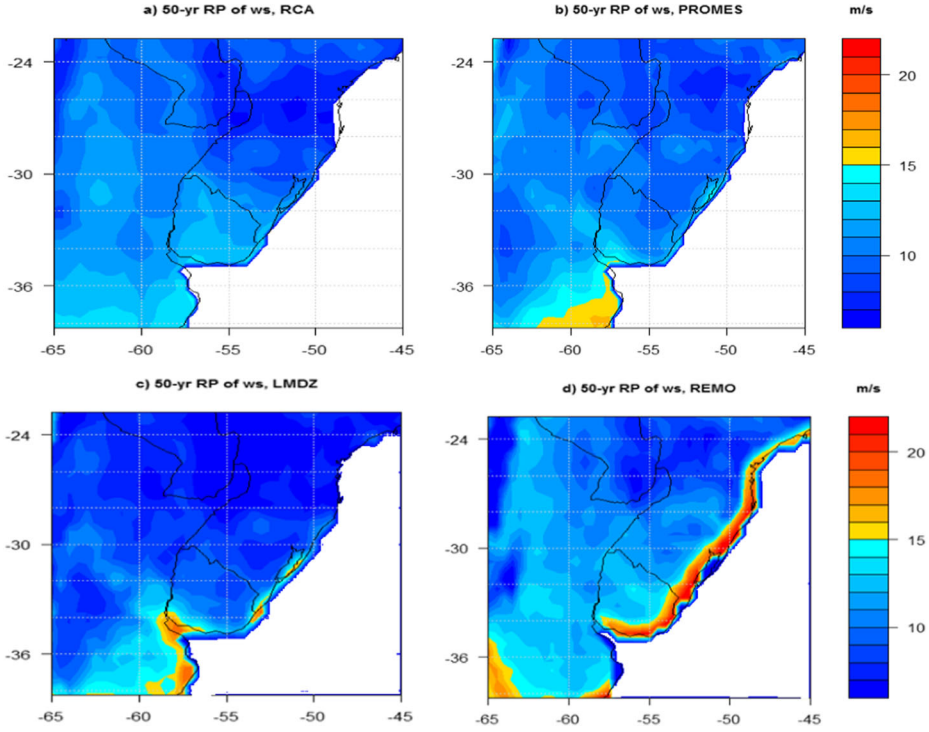

Fig. 6 Wind speed for a 50-year RP calculated from RCMs driven by perfect boundary conditions: **a** RCA, **b** PROMES, **c** LMDZ and **d** REMO. Units are m/s

patterns observed in the benchmark (see Fig. 6 together with Fig. 3a and the high correlation values in Fig. 5), with maximum/minimum values in the south-eastern/north-eastern of SESA. South of about 30°S, all models underestimate the benchmark winds, especially in Buenos Aires province (Argentina) and Uruguay. In the north-western quadrant of the domain, RCA is the only model that captures the footprints of relative maximums and minimums of the benchmark, but not their amplitude. While in the north-eastern quadrant and in agreement with the benchmark, all the models simulate a relative minimum, although they differ in magnitude. As a conclusion, REMO/PROMES is the model that better/worst capture the spatial characteristics of the winds; however, its bias in terms of intensity is relatively large/small (higher than 30%/lower than 10% in vast areas of the region; see Fig. 8 in the Supplementary Material).

On the other hand, although most of models show relatively large biases in winds (as in other variables, see e.g. Menéndez et al. 2016), the 50-year return period calculated by the models fall inside the limits of the benchmark's 95% CI. Note for example, that the RCA wind speed (Fig. 6a) resembles the lower limit of the 95% CI of the benchmark (Fig. 3b); therefore, there is a 95% chance that the maps of wind speed calculated from our climate simulations are correct. This result together with the small spread observed among individual models, give us confidence on the performance of models to assess wind hazard over the SESA domain.

Finally, Carril et al. (2012) and Menéndez et al. (2010) have stressed the benefit of combining CLARIS RCMs in a multi-model ensemble to better reproduce the regional characteristics of the observed mean temperature and precipitation fields. However, return period of 50-year winds calculated from the multi-model ensemble (Fig. 7) keeps the large biases in the coastline of Uruguay and southern Brazil, because it is strongly dependent on the extreme values of the individual simulations. The ensemble gathers the tails of the wind speed distributions in a single distribution, resulting in a curve of return period made up of the highest values of the individual maps. As a consequence, results from the multi-model ensemble are not considered in this study.

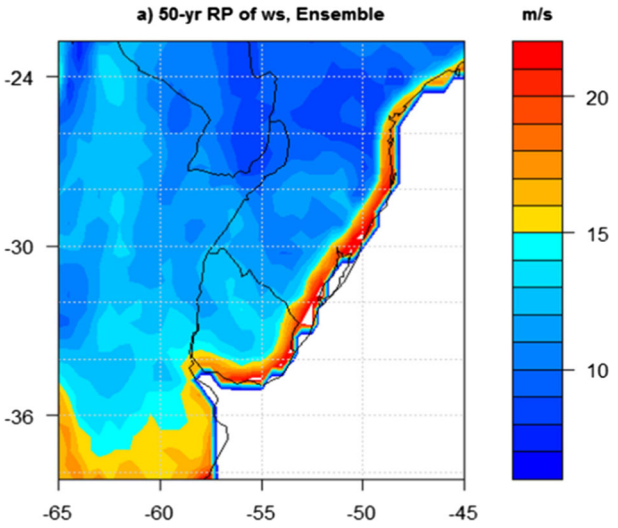

Fig. 7 Wind speed for a 50-year RP calculated from the multi-model ensemble, when models are driven by perfect boundary conditions. Units are m/s

5 Sensitivity to climate change

Sensitivity of winds to climate change in terms of return value is addressed from RCMs-IBC simulations (see Table 1) and summarized in a box-and-whisker plot (Fig. 8). These types of plots are good non-parametric tools to show the distribution of the wind speed quartiles, allowing visually analyzing and comparing various estimators not only the average mean value. Therefore, after computing the 50-year RP from each grid point for current conditions; and for three temporal windows of future climate (near-future 2021–2040, mid-future 2051–2070, and far-future 2081–2100), the variable to compute all statistics is the projected change of wind speed in percentage terms: i.e., for each grid point in SESA, the variable is the projected ws minus the present ws, normalized by the latter. The boxes display the interquartile range (i.e., 25th–75th quartile distance; IQR), the black bar (white star) within the boxes is the mean (median) value, whiskers extend up to 1.5 times the size of the IQR, and values exceeding whiskers are outliers.

The figure gives us insights about how the models project the changes in the spatial statistical distribution of the wind speed (in terms of 50-year RP) within SESA. The changes projected by four models give us a measure of the uncertainty related to the model spread. Although projected changes are small, in terms of mean and median values over SESA, three of four models project decreases of ws (up to the 5%) along the twenty-first century. The magnitude of the change with respect to the current climate amplifies with time, strengthening confidence in far-future projections. Climate change sensitivity in terms of IQR values is always lower than 10%, while sensitivity of whiskers is up to 22%. In this ensemble, LMDZ is the outlier model, projecting increases of ws along the twenty-first century, modulated by signal of inter-decadal variability. The inter-model spread, which is manifested at the

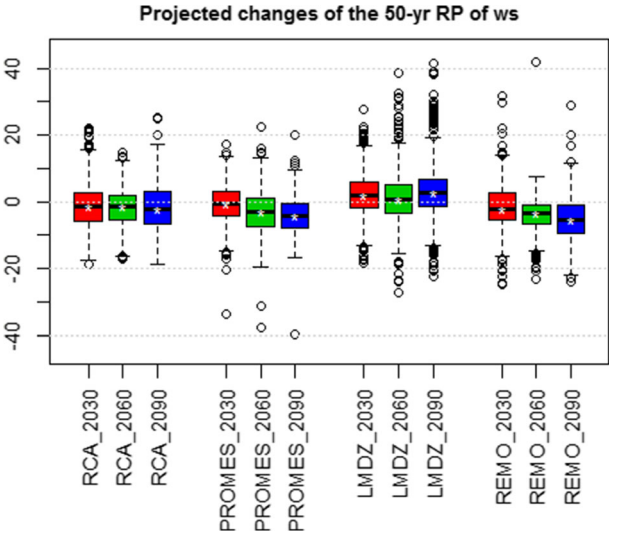

Fig. 8 Sensitivity of wind speed to climate change for three 20-year windows: 2021–2040 (in red), 2051–2070 (in green), and 2081–2100 (in blue). The diagram shows the change of wind speed (%) with respect to current climate over the SESA domain. Each box represents the interquartile distance (IQD). The mean value is indicated by the black wide line and the median by the star inside the boxes. Values more than 1.5 times the IQD are considered outliers (black circles)

individual grid-point level and therefore in the spatial statistical distribution displayed in Fig. 8, may reflect differences in models physics but also in the vertical interpolation.

6 Conclusions and future work

In this work, we have presented maps of return period of wind speed as a first step in the study of wind hazard in South Eastern South America. To overcome the limitations of wind recording stations, the wind hazard maps were generated from wind extracted from climate simulations. Simulations from four models (RCA, PROMES, LMDZ and REMO) forced by ERA Interim reanalysis and by a set of global climate change experiments were available for this project.

The quality of climate simulations in terms of wind speed was assessed against the reanalysis by calculating a number of RP using data over the 1991–2010 interval (current climate conditions). The performance of the models was satisfactory. The simulations used here match the spatial patterns of the benchmark winds maps (with relative maximum values occurring in the south-eastern of SESA and relative minimum values in the north-eastern sector) and simulated wind speeds fall inside the limits of the benchmark's 95% CI. The analysis shows that RCMs are appropriate to assess wind hazard over SESA.

The mean climate change signal of the wind speeds is within 5% of the value for current climate, and close to the 10% in terms of IQR. Sensitivity is small compared with the uncertainty: (i) changes in outliers are larger than 40% evidencing strong changes in the variability; (ii) although dispersion among models is small when simulating the current wind speed fields, the spread of the inter-model signal of climate change adds an extra source of uncertainty. Three models project lower wind speeds for future climate, while the fourth one projects wind increases by the end of the twenty-first century and adds uncertainty regarding the relative signal of the climate change condition vs. the inter-decadal internal variability. Our results show that we could expect little variation in wind speed over the SESA region for most of this century. Similar results on a world-wide scale are reported by Watson (2014).

Sensitivity of wind speed to time of the year was examined by calculating seasonal return period of wind speed. The results show that wind hazard is not very sensitive to seasonal considerations; this is because wind hazard is strongly dependent on extremes and they can happen any time of the year.

The maps presented here were calculated from *mean* wind speeds whilst the interest of emergency and planning authorities is in maps of *gust* winds. These types of winds can be calculated from the mean winds multiplying by a Gust Factor (GF). Calculation of the GF for a number of regions in SESA requires reliable records of hourly wind speeds ((Halfdan and Haraldur 2004; Cheng et al. 2012). We are working on the available records to select a subset of good-quality wind data for GF calculation. In future, we expect to calculate the corresponding maps of gust winds.

Another area of improvement for this project is to increase the number of RCMs. The four models used here provide an initial assessment of the problem but more definitive results requires a lot more models. We hope to be able to add results to the project from more models as soon as they are available. We also hope that some of these models will provide simulations at higher resolutions in order to give more detail to the distribution of winds over the SESA region.

Acknowledgements We acknowledge the CLARIS-LPB project for providing the data from the regional climate models. The authors wish to thank our colleague G. Pita (Johns Hopkins University, USA) and three anonymous referees for their comments and helpful advice to improve the paper.

Funding information This research was supported by ANPCyT (PICT-2015-3097 and PICT-2014-0887) and CONICET (PIP-112-2015-0100402CO). The stage of L.A. Sanabria in Argentina was supported by the program "Stays for foreign researchers and/or experts during sabbatical periods," CONICET, Argentina. Thanks to our colleague Bruno Natalini (UNNE) for developing the application.

References

Bao X, Zhang F (2013) Evaluation of NCEP–CFSR, NCEP–NCAR, ERA-interim, and ERA-40 reanalysis datasets against independent sounding observations over the Tibetan Plateau. J Clim 26:206–214

Boulanger JP, Brasseur G, Carril AF et al (2010) A Europe–South America network for climate change assessment and impact studies. Clim Chang 98:307–329. https://doi.org/10.1007/s10584-009-9734-8

Boulanger JP, Carril AF, Sanchez E (2016) CLARIS-La Plata Basin: regional hydroclimate variability, uncertainties and climate change scenarios. Clim Res 68:93–94. https://doi.org/10.3354/cr01392

Brower MC (2013) A study of wind speed variability using global reanalysis data. AWS Truepower, LLC, Albany

Carril AF, Menéndez CG et al (2012) Performance of a multi-RCM ensemble for South Eastern South America. Clim Dyn 39:2747–2768. https://doi.org/10.1007/s00382-012-1573-z

Carril AF, Cavalcanti IFA, Menéndez CG et al (2016) Extreme events in the La Plata basin: a retrospective analysis of what we have learned during CLARIS-LPB project. Clim Res 68:95–116. https://doi.org/10.3354/cr01374

Cavalcanti IFA, Carril AF, Penalba OC et al (2015) Precipitation extremes over La Plata Basin—review and new results from observations and climate simulations. J Hydrol 523:211–230. https://doi.org/10.1016/j.jhydrol.2015.01.028

Cechet R.P., Sanabria L.A., Divi C.B., Thomas C., Yang T., et al (2012) Climate Futures for Tasmania: severe wind hazard and risk technical report, Geoscience Australia Record 2012/43

Cheng CS, Li G, Li Q, Auld H, Fu C (2012) Possible impacts of climate change on wind gusts under downscaled future climate conditions over Ontario, Canada. J Clim 25:3390–3408. https://doi.org/10.1175/JCLI-D-11-00198.1

Coles S (2001) An introduction to statistical modeling of extreme values. Springer, London

Cvitan L (2003) Determining wind gusts using mean hourly wind speed. Geofizika 20:63–74

Dee DP, Uppala SM, Simmons AJ et al (2011) The ERA-Interim reanalysis: configuration and performance of the data assimilation system. Q J R Meteorol Soc 137:553–597. https://doi.org/10.1002/qj.828

Durañona V (2015) Extreme Wind climate of Uruguay. Ph.D. Thesis. Facultad de Ingenieria, Universidad de la Republica. Montevideo. Uruguay

Ferreira V, Nascimento EL (2016) Convectively-induced severe wind gusts in southern Brazil: surface observations, atmospheric environment, and association with distinct convective modes. 28th Conference on Severe Local Storms. 7–11 November 2016 Portland, OR, USA

Garreaud RD, Vuille M, Compagnucci R, Marengo J (2009) Present-day South American climate. Palaeogeogr Palaeoclimatol Palaeoecol 281(2009):180–195

Gatey DA (2011) The analysis of extreme synoptic winds. Ph.D. Thesis. Western University. Electronic Thesis and Dissertation Repository. 268. http://ir.lib.uwo.ca/etd/268

Gilleland E, Katz RW (2005) Analysing seasonal to interannual extreme weather and climate variability with the extremes toolkit. National Center for Atmospheric. Research (NCAR), Boulder

Gilleland E, Katz RW (2011) New software to analyze how extremes change over time. Eos 92(2):13–14

Giorgi F (2006) Regional climate modeling: status and perspectives. J Phys IV France 139(101):118. https://doi.org/10.1051/jp4:2006139008

Giorgi F, Jones C, Asrar GR (2009) Addressing climate information needs at the regional level: the CORDEX framework. Bull World Meteorol Organ 58:175–183

Halfdan A, Haraldur O (2004) Mean gust factors in complex terrain. Meteorol Z 13(2):149–155 (in English)

Holmes JD (2007) Wind Loading of Structures. Taylor & Francis

Holmes JD, Moriarty WW (1999) Application of the generalised Pareto distribution to extreme value analysis in wind engineering. J Wind Eng Indus Aerodyn 83:1–10

Katz RW (2013) Statistical methods for nonstationary extremes. In: AghaKouchak A, Easterling D, Hsu K, Schubert S, Sorooshian S (Eds.) Extremes in a changing climate. Detection, Analysis and Uncertainty. Springer

Kunz M, Mohr S, Rauthe M, Luz R, Kottmeier C (2010) Assessment of extreme wind speeds from regional climate models—part 1: estimation of return values and their evaluation. Nat Hazards Earth Syst Sci 10:907–922

Liléo S, Berge E, Undheim O, Klinkert R, Bredesen RE (2013) Long-term correction of wind measurements. State-of-the-art, guidelines and future work. Elforsk report 13:18

López-Franca N, Zaninelli PPG, Carril AA, Menéndez CG, Sánchez E (2016) Changes in temperature extremes for 21st century scenarios over South America derived from a multi-model ensemble of regional climate models. Clim Res 68:151–167. https://doi.org/10.3354/cr01393 http://www.int-res.com/abstracts/cr/v68/n2-3/p151-167/ (Accessed September 23, 2016)

Menéndez CG, De Castro M, Sörensson A, Boulanger JP (2010) CLARIS project: towards climate downscaling in South America. Meteorol Zeitschrift 19:357–362. https://doi.org/10.1127/0941-2948/2010/0459

Menéndez CG, Zaninelli PG, Carril AF, Sánchez E (2016) Hydrological cycle, temperature, and land surface-atmosphere interaction in the La Plata Basin during summer: response to climate change. Clim Res. https://doi.org/10.3354/cr01373

Nakicenovic N, Alcamo J, Grubler A, Riahi K, Roehrl RA, Rogner HH, Victor N (2000) Special report on emissions scenarios (SRES), A Special Report of Working Group III of the Intergovernmental Panel on Climate Change. Cambridge University Press, 599 pp

Natalini BM, Natalini B, Atencio BA, Zaracho JI (2016) Análisis de velocidades de viento extremas de 11 estaciones en Argentina – perspectivas para una actualización del mapa de vientos extremos. Proceedings of the XXIV Jornadas Argentinas de Ingeniería Estructural, Buenos Aires, Sept 28-30

Pita G, Schwarzkopf MLA (2016) Urban downburst vulnerability and damage assessment from a case study in Argentina. Nat Hazards. https://doi.org/10.1007/s11069-016-2323-z

Pryor SC, Barthelmie RJ, Clausen NE et al (2012) Analyses of possible changes in intense and extreme wind speeds over northern Europe under climate change scenarios. Clim Dyn 38:189. https://doi.org/10.1007/s00382-010-0955-3

Rockel B, Woth K (2007) Extremes of near-surface wind speed over Europe and their future changes as estimated from an ensemble of RCM simulations. Clim Chang 81(Suppl 1):267. https://doi.org/10.1007/s10584-006-9227-y

Sanabria LA, Cechet RP (2007) A Statistical Model of Severe Winds. Geoscience Australia. GeoCat # 65052 http://ga.gov.au/hazards/severe-weather/reports.html (accessed May 2016)

Sánchez E, Solman S, Remedio ARC, Berbery H, Samuelsson P, Da Rocha RP, Mourão C, Li L, Marengo J, de Castro M, Jacob D (2015) Regional climate modelling in CLARIS-LPB: a concerted approach towards twentyfirst century projections of regional temperature and precipitation over South America. Clim Dyn. https://doi.org/10.1007/s00382-014-2466-0

Solman SA (2016) Systematic temperature and precipitation biases in the CLARIS-LPB ensemble simulations over South America and possible implications for climate projections. Clim Res. https://doi.org/10.3354/cr01362

Solman SA, Sanchez E, Samuelsson P et al (2013) Evaluation of an ensemble of regional climate model simulations over South America driven by the ERA-Interim reanalysis: model performance and uncertainties. Clim Dyn 41:1–19. https://doi.org/10.1007/s00382-013-1667-2

Song L, Liu Z, Wang F (2015) Comparison of wind data from ERA-Interim buoys in the Yellow and East China Seas. Chin J Oceanol Limnol 33(1):282–288

Taylor KE (2001) J Geophys Res 106(D7):7183–7192

Wang CH, Wang X, Khoo YB (2013) Extreme wind gust hazard in Australia and its sensitivity to climate change. Nat Hazards 67:549. https://doi.org/10.1007/s11069-013-0582-5

Watson SJ (2014) Quantifying the variability of wind energy. Wiley Interdiscip Rev: Energy Environ 3(4):330–342

Zhang X, Zwiers FW (2013) Statistical indices for the diagnosing and detecting changes in extremes. In: AghaKouchak A, Easterling D, Hsu K, Schubert S, Sorooshian S Eds. Extremes in a changing climate, detection, analysis and uncertainty. Springer

Zipser EJ et al (2006) Where are the most intense thunderstorms on earth? BAMS. doi:https://doi.org/10.1175/BAMS-87-8-1057